Supporting Information for "Evaluating the water cycle over CONUS at the watershed scale for the Energy Exascale Earth System Model version 1 (E3SMv1) across resolutions"

Bryce E. Harrop[1], Karthik Balaguru[1], Jean-Christophe Golaz[2],

L. Ruby Leung[1], Salil Mahajan[3], Alan M. Rhoades[4], Paul A. Ullrich[5],

Chengzhu Zhang[2], Xue Zheng[2], Tian Zhou[1], Peter M. Caldwell[2],

Noel D. Keen[4], Azamat Mametjanov[6]

[1]Pacific Northwest National Laboratory, Richland, WA, USA

[2]Lawrence Livermore National Laboratory, Livermore, CA, USA

[3]Oak Ridge National Laboratory, Oak Ridge, TN, USA

[4]Lawrence Berkeley National Laboratory, Berkeley, CA, USA

[5]Department of Land, Air, and Water Resources, University of California-Davis, Davis, CA, USA

[6]Argonne National Laboratory, Lemont, IL, USA

Contents of this file

Summary The following material provides additional results meant to supplement those presented within the main manuscript. Figures include the full seasonal cycle of each water budget term for all of the CONUS HUC2 watersheds, the streamflow sensitivity for

each watershed, as well as several other figures that provide insight into the water cycle changes between HR and LR.

References

Golaz, J., Caldwell, P. M., Van Roekel, L. P., Petersen, M. R., Tang, Q., Wolfe, J. D., ... Zhu, Q. (2019). The DOE E3SM coupled model version 1: Overview and evaluation at standard resolution. *Journal of Advances in Modeling Earth Systems*. doi: 10.1029/2018ms001603

	Eastern CONUS			Central CONUS			Western CONUS		
HUC2 Region	LR	HR	ERA5	LR	HR	ERA5	LR	HR	ERA5
Tropical Cyclones	1.7%	6.5%	4.7%	0.5%	2.0%	1.6%	0.0%	0.0%	0.1%
Atmospheric Rivers	30.5%	26.5%	29.4%	13.0%	12.5%	17.1%	5.2%	4.6%	3.0%
Extratropical Cyclones	6.9%	5.9%	5.6%	8.9%	12.7%	8.4%	9.6%	19.4%	18.8%
Residual	60.9%	61.1%	60.3%	77.5%	72.8%	72.9%	85.2%	76.0%	78.1%
Normalized SDI	0.66	0.72	0.70	0.51	0.60	0.58	0.47	0.61	0.56

Table S1. Percentage contribution to precipitation totals in each CONUS region, filtered by associated features. For the Eastern and Central CONUS, the averaging time period is June-September, while for the Western CONUS, the averaging time period is April-July. These time periods are consistent with the analysis in section 3.2.

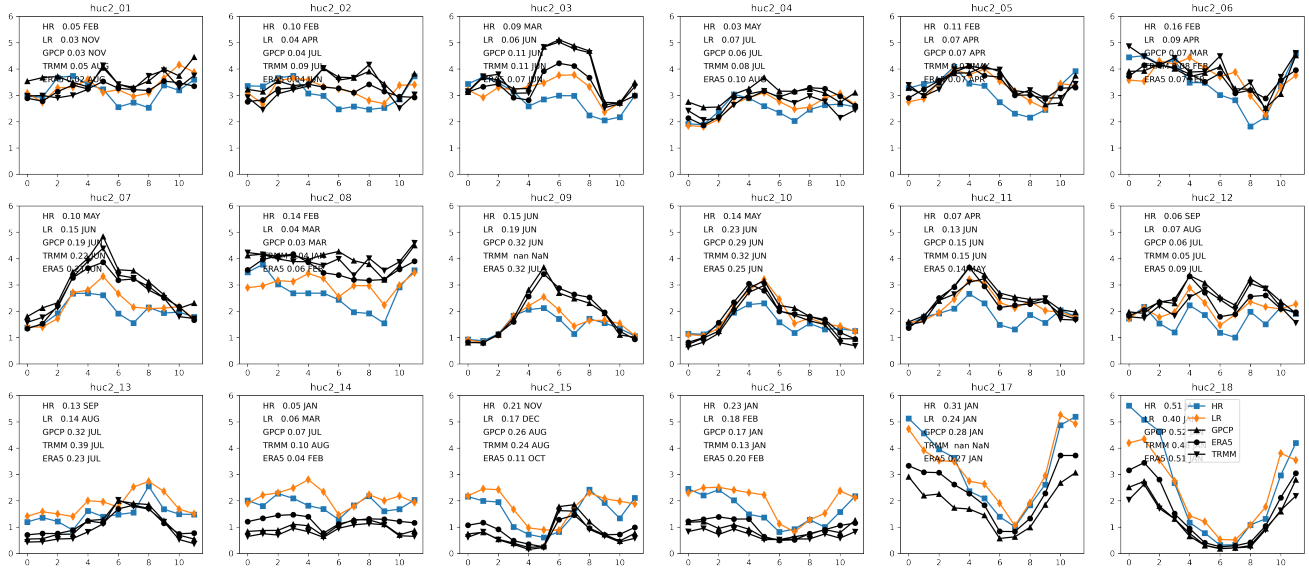

Figure S1. Seasonal timeseries of precipitation for HR (blue), LR (orange), and observational and reanalysis datasets (black) for each watershed (panels). The numbers in each panel provide the amplitude of the first Fourier mode, denoting the amplitude of the seasonal cycle. The month denotes the phase of the seasonal cycle.

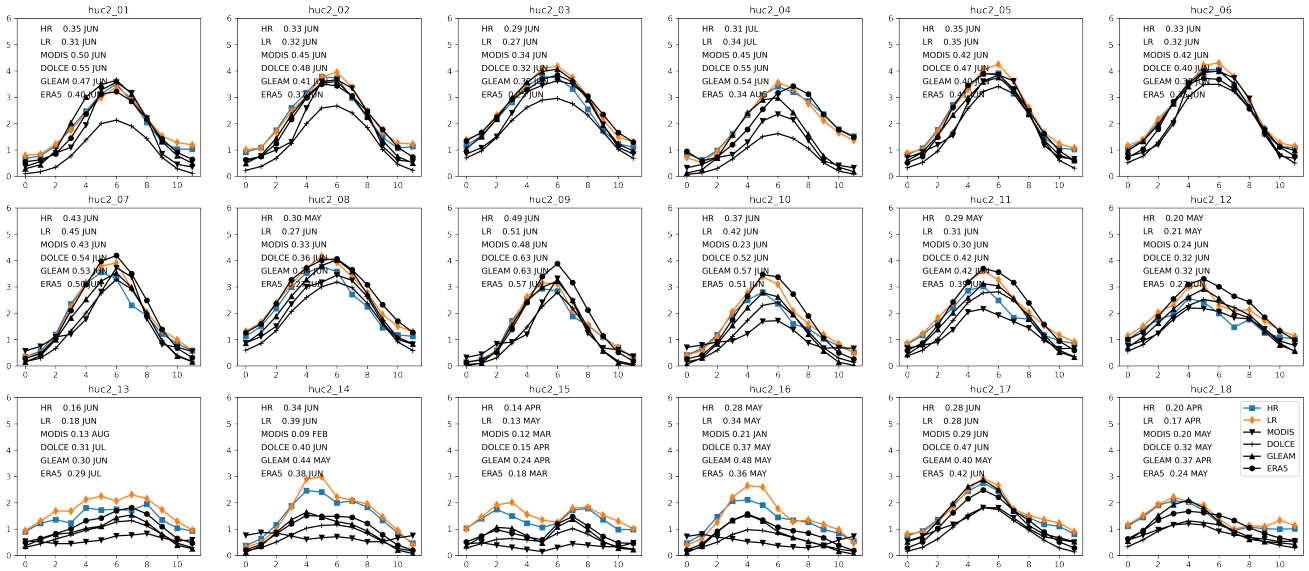

Figure S2. Seasonal timeseries of evapotranspiration for HR (blue), LR (orange), and observational and reanalysis datasets (black) for each watershed (panels). The numbers in each panel provide the amplitude of the first Fourier mode, denoting the amplitude of the seasonal cycle. The month denotes the phase of the seasonal cycle.

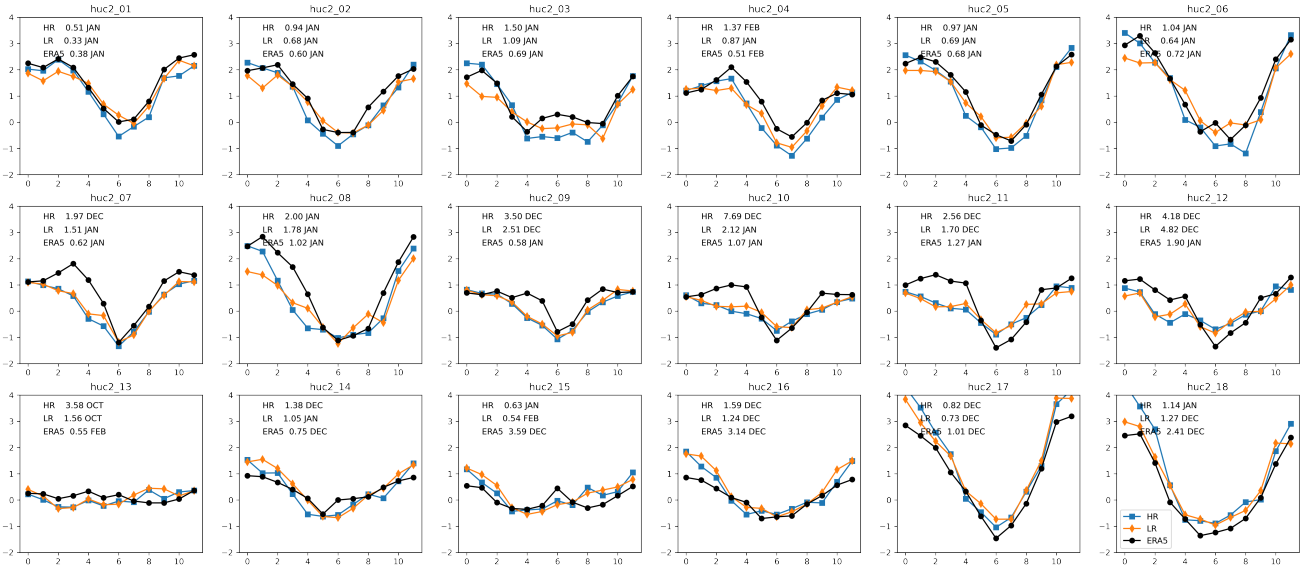

Figure S3. Seasonal timeseries of moisture convergence for HR (blue), LR (orange), and observational and reanalysis datasets (black) for each watershed (panels). The numbers in each panel provide the amplitude of the first Fourier mode, denoting the amplitude of the seasonal cycle. The month denotes the phase of the seasonal cycle.

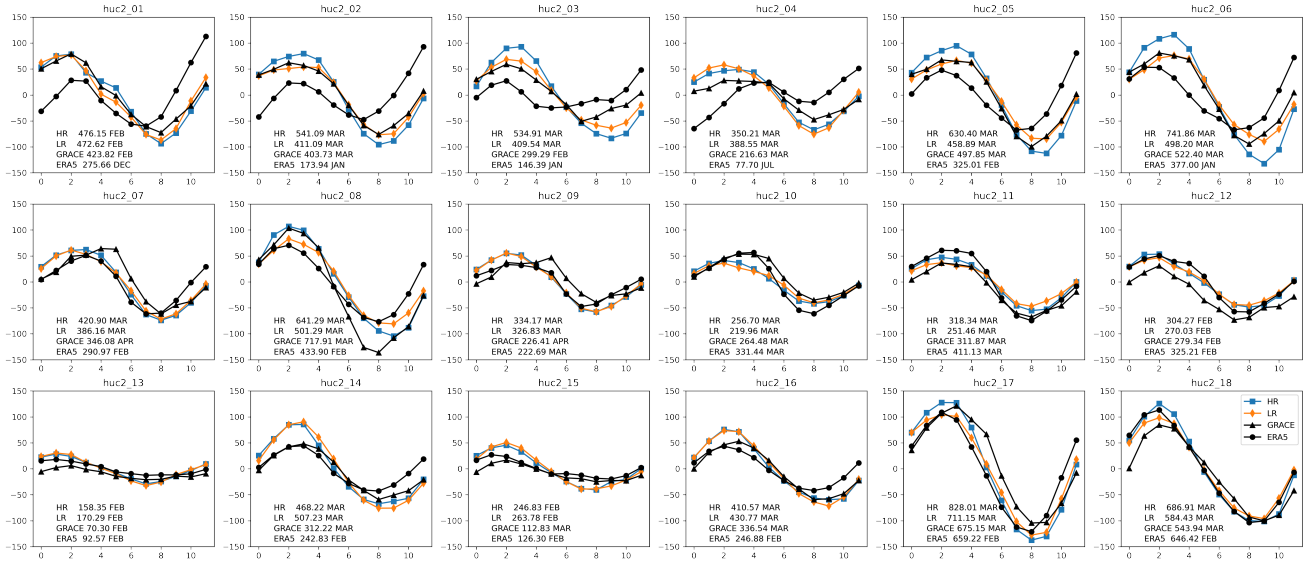

Figure S4. Seasonal timeseries of terrestrial water storage anomaly for HR (blue), LR (orange), and observational and reanalysis datasets (black) for each watershed (panels). The numbers in each panel provide the amplitude of the first Fourier mode, denoting the amplitude of the seasonal cycle. The month denotes the phase of the seasonal cycle.

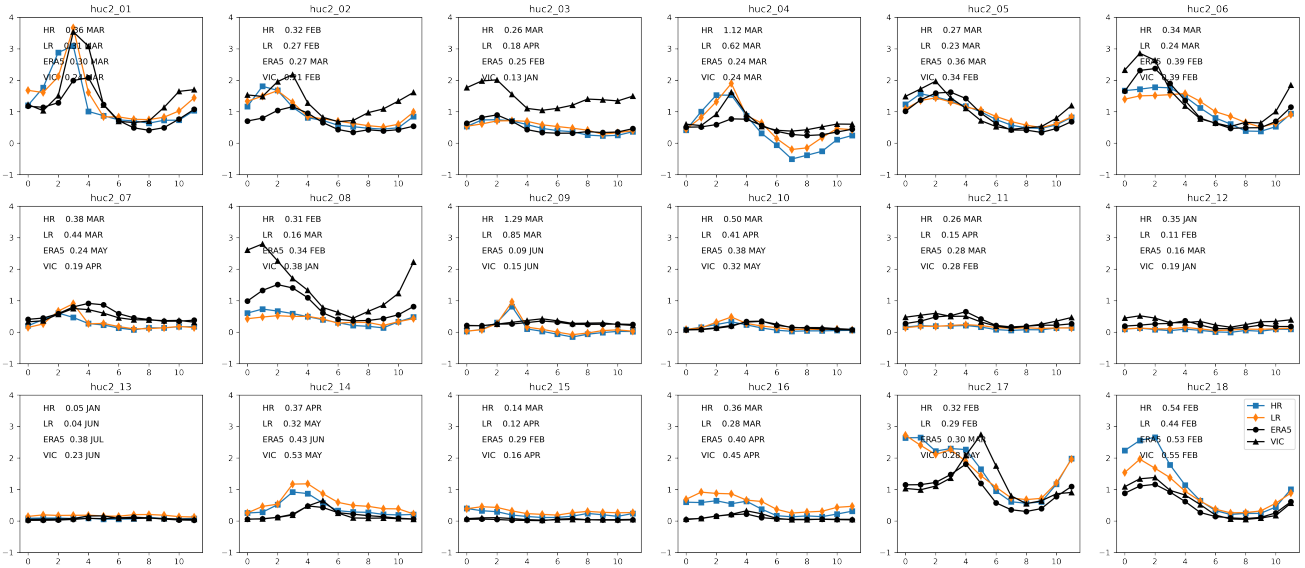

Figure S5. Seasonal timeseries of runoff (combined surface and sub-surface) for HR (blue), LR (orange), and observational and reanalysis datasets (black) for each watershed (panels). The numbers in each panel provide the amplitude of the first Fourier mode, denoting the amplitude of the seasonal cycle. The month denotes the phase of the seasonal cycle.

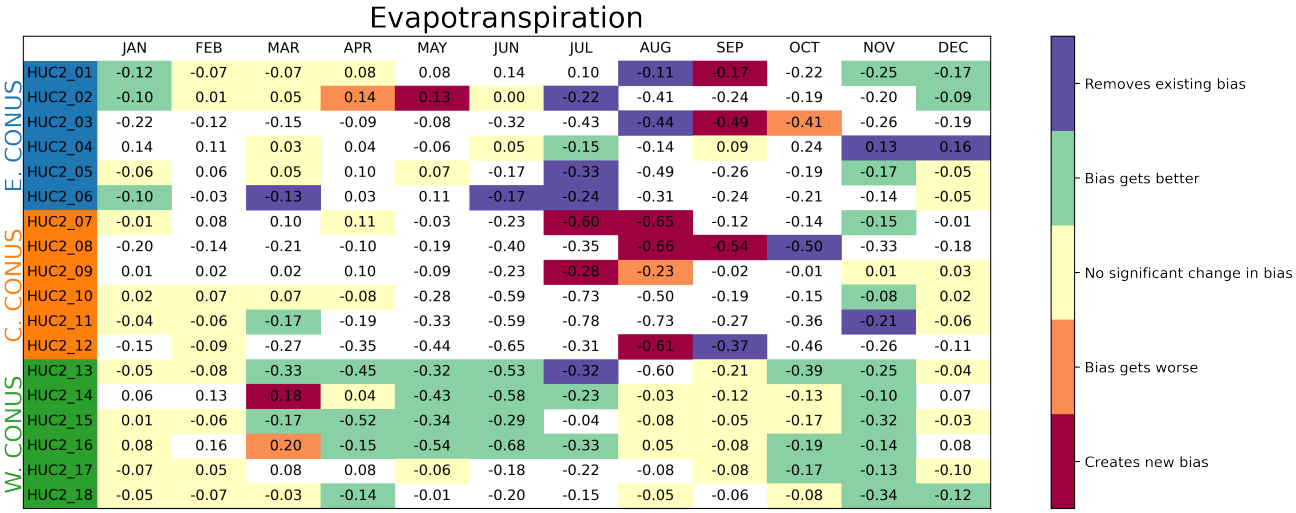

Figure S6. Stoplight diagram for evapotranspiration. Each column represents a month and each row a HUC2 watershed. The values in each cell are the mean difference between LR and HR (HR - LR). White denotes a month where no significant bias exists between either LR or HR with the observations. Yellow denotes months where no significant bias exists between LR and HR, but both are significantly biased relative to observations. Purple denotes months where LR is biased relative to observations, while HR is not. Green denotes months where LR is biased relative to observations and HR makes a significant improvement upon that bias. Orange denotes the opposite of green – both LR and HR are biased against observations, but the bias is significantly larger in HR than in LR. Finally, red denotes regions where no bias exists for LR, but a bias does occur for HR. Statistical significance is determined using a t-test with a 95% significance threshold and treating each year as an independent sample for a particular basin and month. Comparison datasets for evapotranspiration include MODIS, GLEAM, and ERA5, but do not include DOLCE.

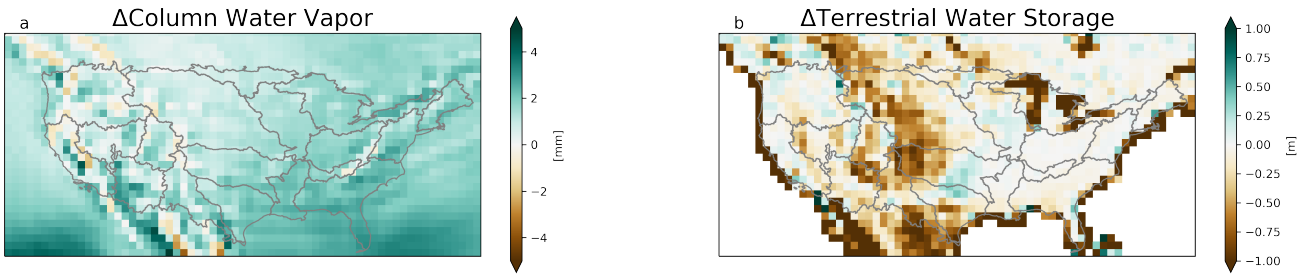

Figure S7. Changes in column water vapor (a) and terrestrial water storage (b) going from LR to HR. Both HR and LR are remapped to a regular 1x1 degree lat-lon grid for comparison. The remapping from the different land meshes creates noise around the coastlines which should be ignored when comparing the differences.

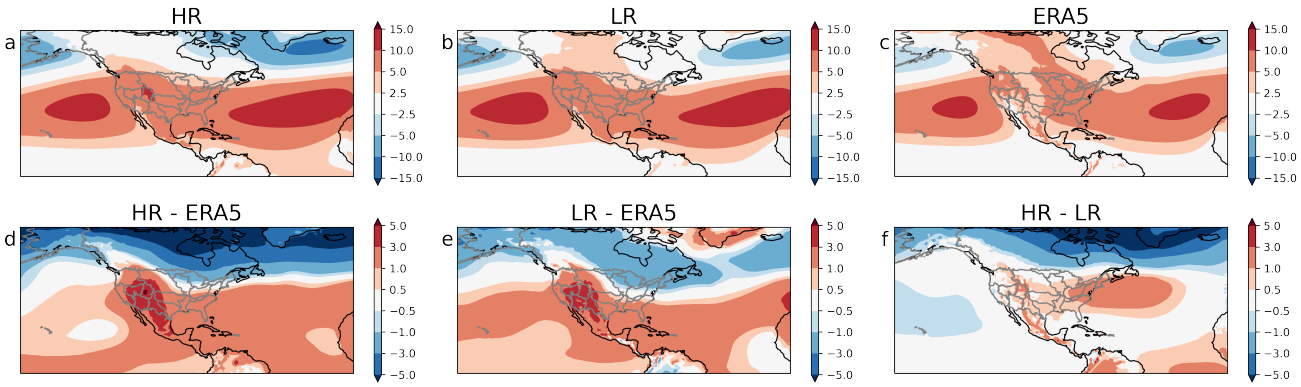

Figure S8. Surface pressure (with global mean subtracted) for (a) HR, (b) LR, and (c) ERA5. Differences between (d) HR and ERA5, (e) LR and ERA5, and (f) HR and LR are shown in the bottom row. All values are given in units of hPa.

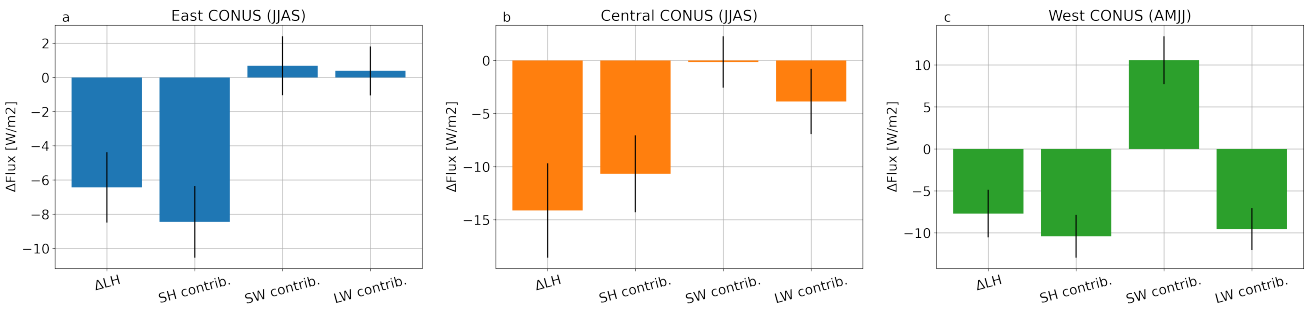

Figure S9. Mean difference in latent heat between LR and HR, and contributions to that difference from sensible heat flux, surface net shortwave radiative flux, and surface net longwave radiative flux for (a) Eastern CONUS, (b) Central CONUS, and (c) Western CONUS. The error bars provide the 95% confidence interval for the mean differences.

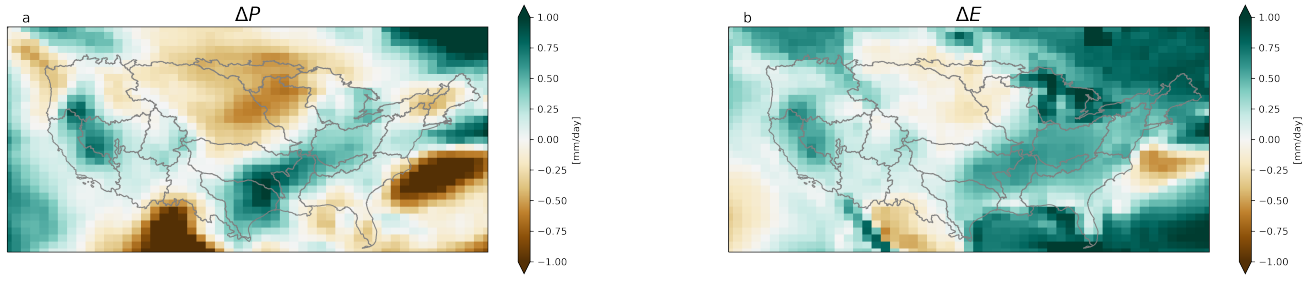

Figure S10. Changes in precipitation (a) and evapotranspiration (b) between the piControl and abrupt4xCO2 E3SMv1 experiments detailed by Golaz et al. (2019).

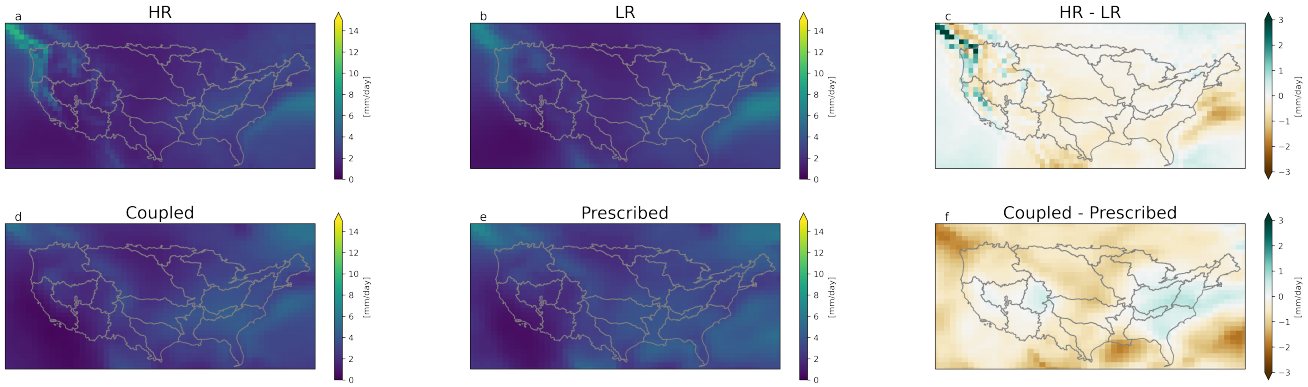

Figure S11. Precipitation for HR (a), LR (b), the fully coupled abrupt4xCO2 experiment (d), and an experiment with SSTs prescribed from the abrupt4xCO2 experiment (e). Panel c shows the difference in precipitation between HR and LR, and panel f shows the difference in precipitation between interactive and prescribed SSTs.

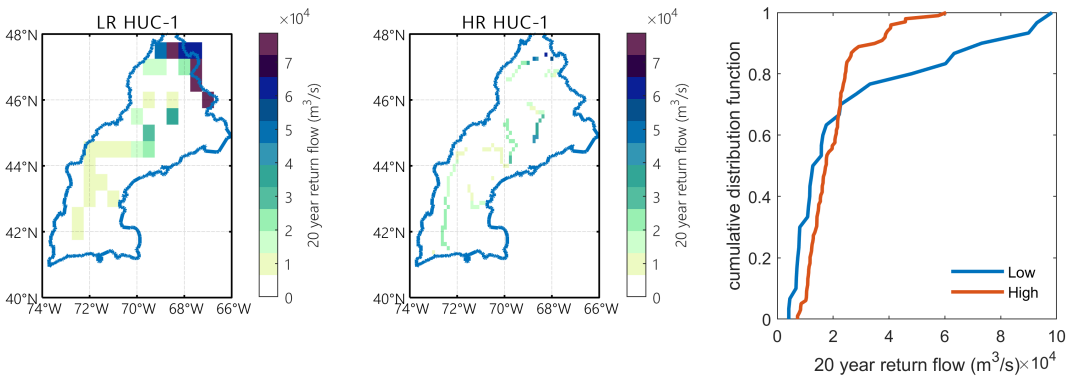

Figure S12. Simulated 20-year return streamflow for low resolution (Left) and high resolution (Middle), and the comparison of the cumulative distribution functions (CDFs) between HR and LR (Right) for the New England (1) region.

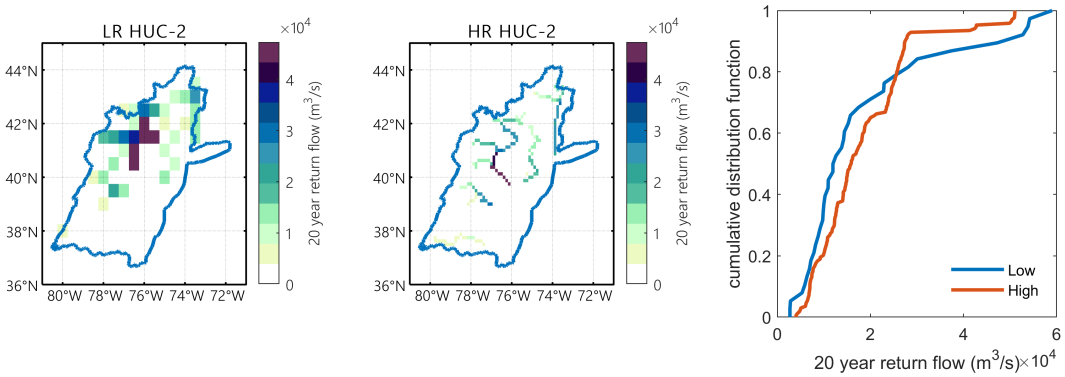

Figure S13. Same as Figure S12, only for the Mid Atlantic (2) region.

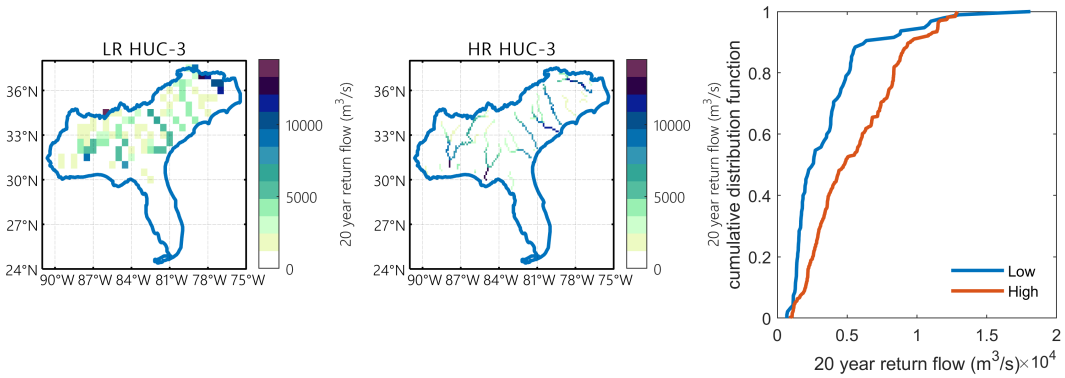

Figure S14. Same as Figure S12, only for the South Atlantic-Gulf (3) region.

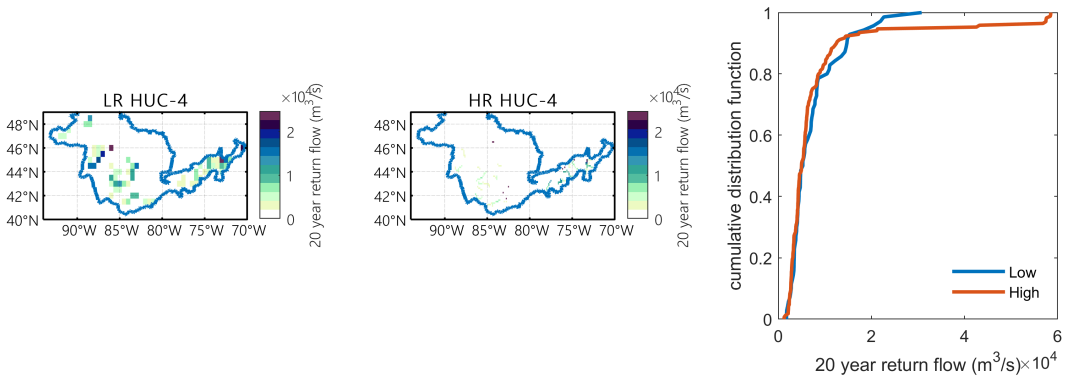

Figure S15. Same as Figure S12, only for the Great Lakes (4) region.

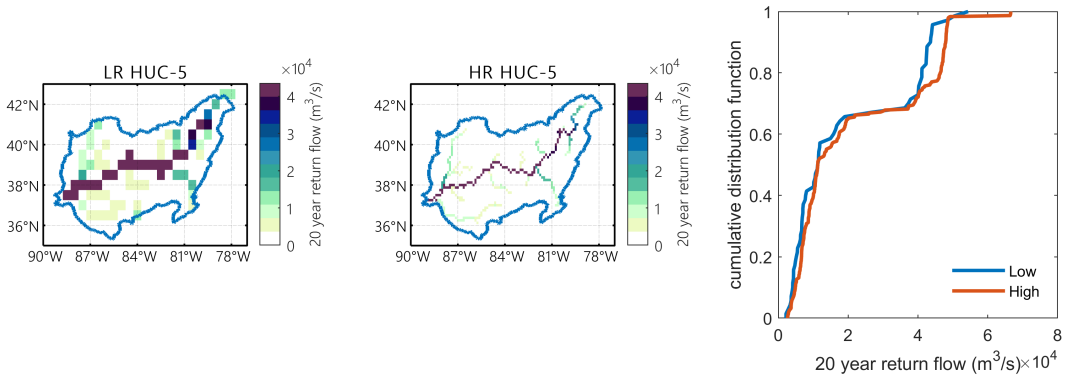

Figure S16. Same as Figure S12, only for the Ohio (5) region.

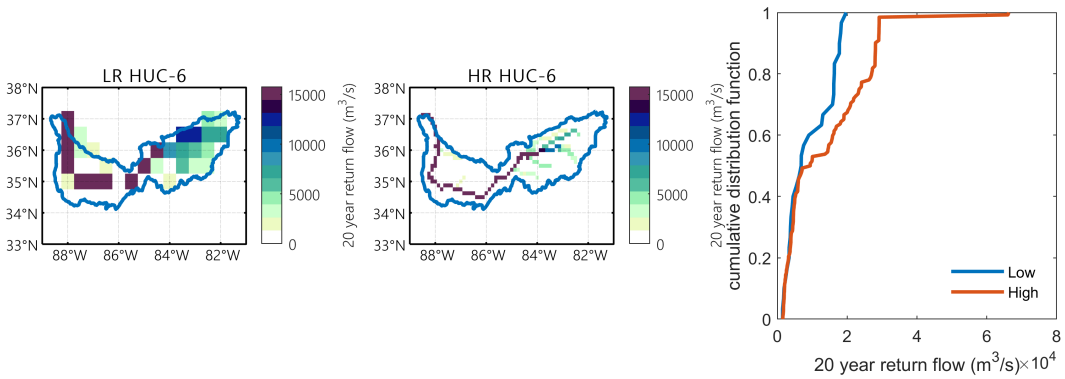

Figure S17. Same as Figure S12, only for the Tennessee (6) region.

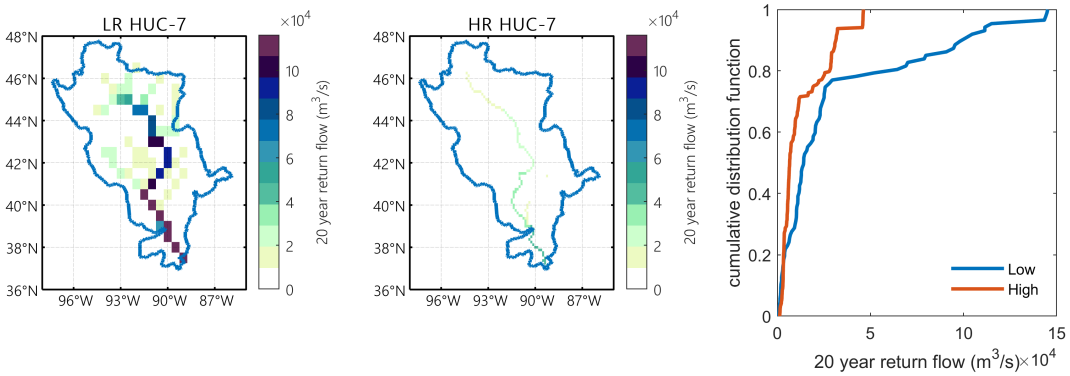

Figure S18. Same as Figure S12, only for the Upper Mississippi (7) region.

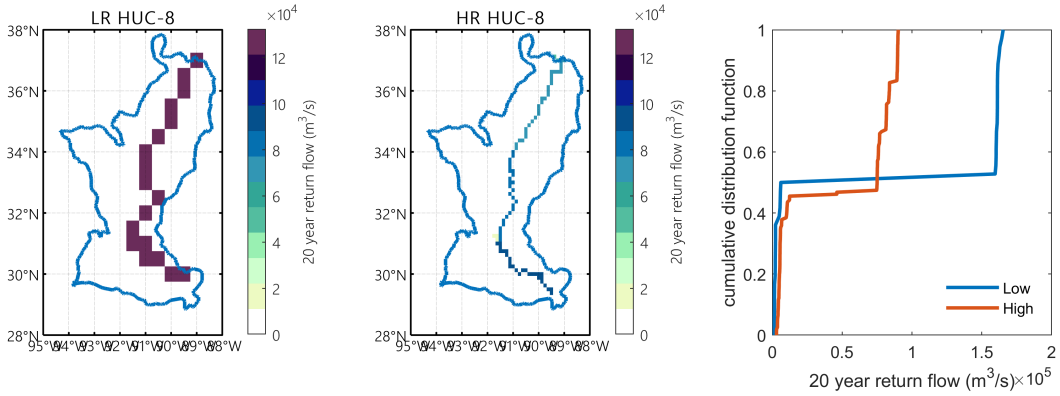

Figure S19. Same as Figure S12, only for the Lower Mississippi (8) region.

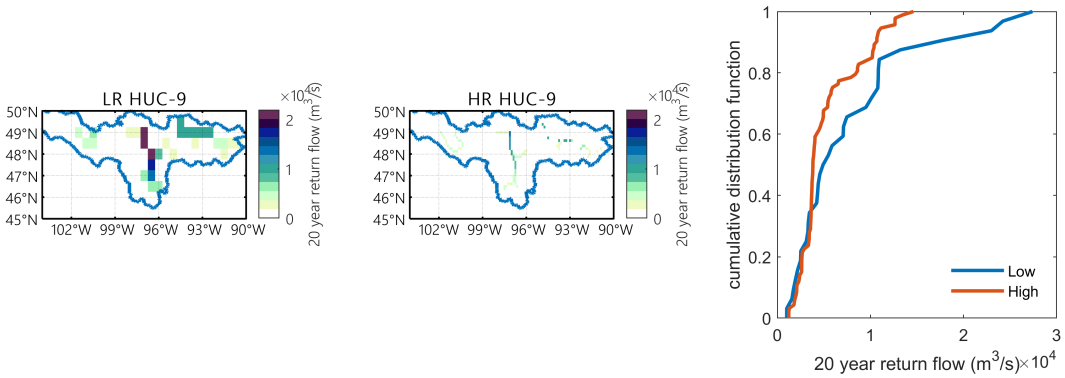

Figure S20. Same as Figure S12, only for the Souris-Red-Rainy (9) region.

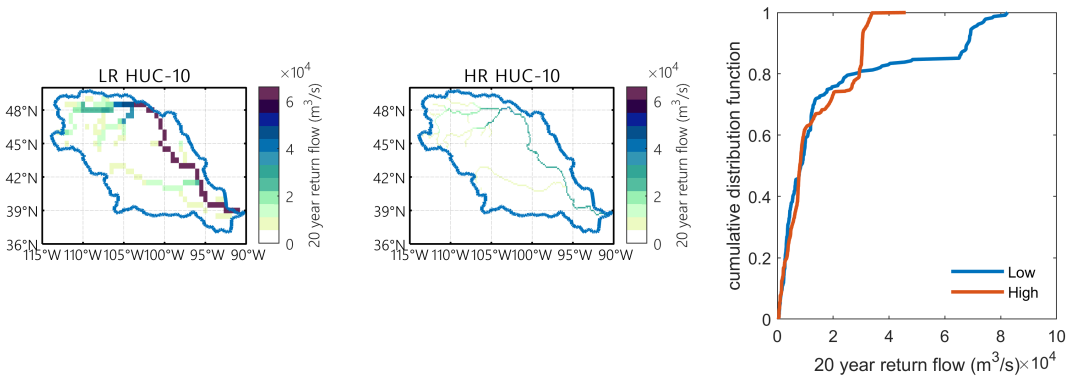

Figure S21. Same as Figure S12, only for the Missouri (10) region.

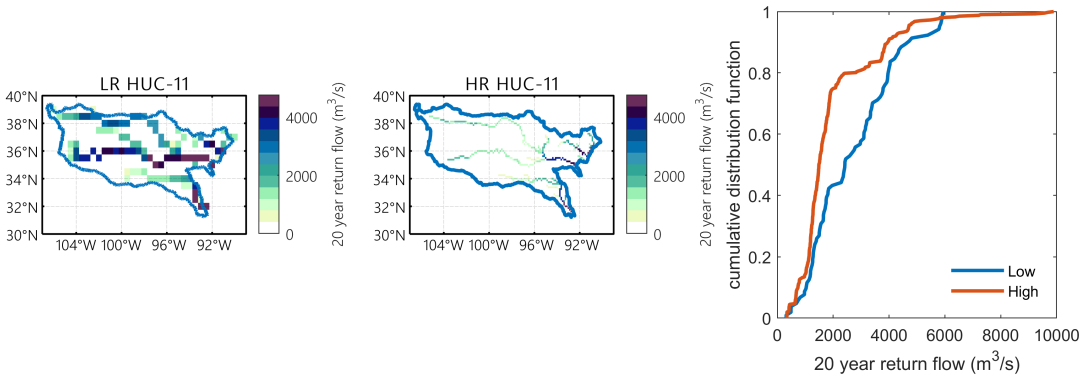

Figure S22. Same as Figure S12, only for the Arkansas-White-Red (11) region.

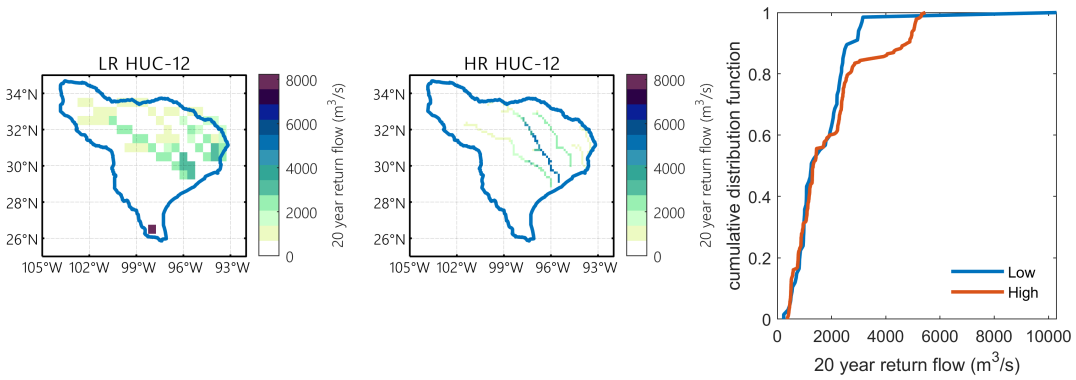

Figure S23. Same as Figure S12, only for the Texas-Gulf (12) region.

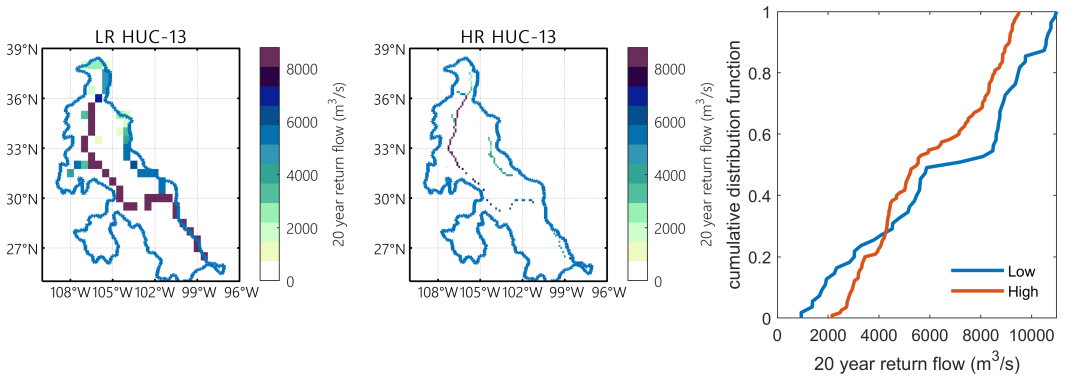

Figure S24. Same as Figure S12, only for the Rio Grande (13) region.

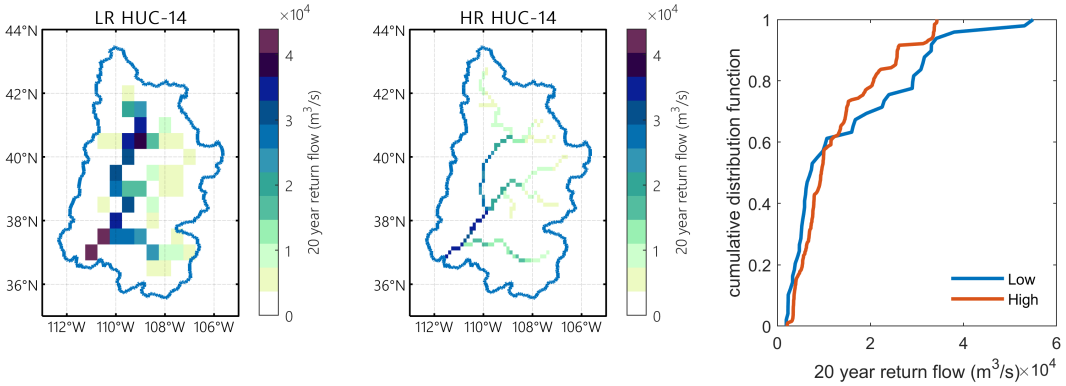

Figure S25. Same as Figure S12, only for the Upper Colorado (14) region.

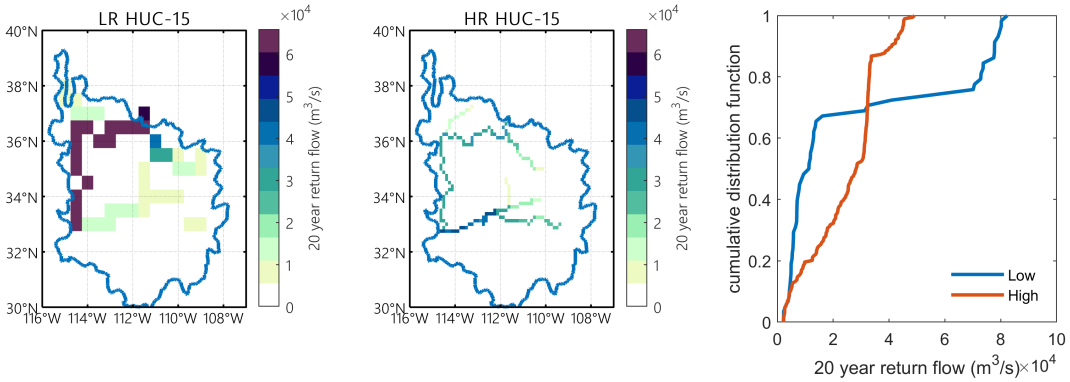

Figure S26. Same as Figure S12, only for the Lower Colorado (15) region.

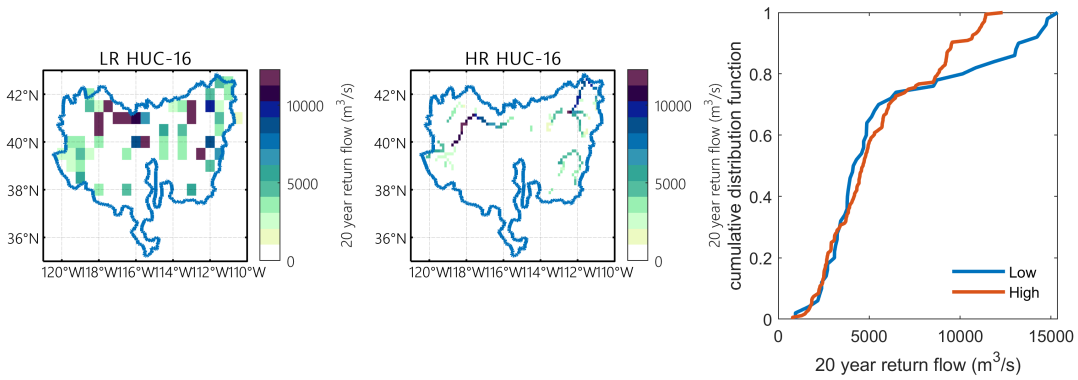

Figure S27. Same as Figure S12, only for the Great Basin (16) region.

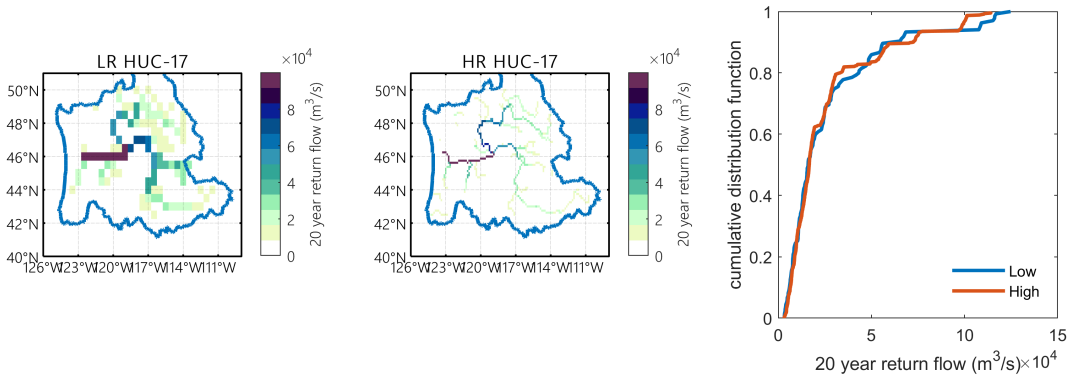

Figure S28. Same as Figure S12, only for the Pacific Northwest (17) region.

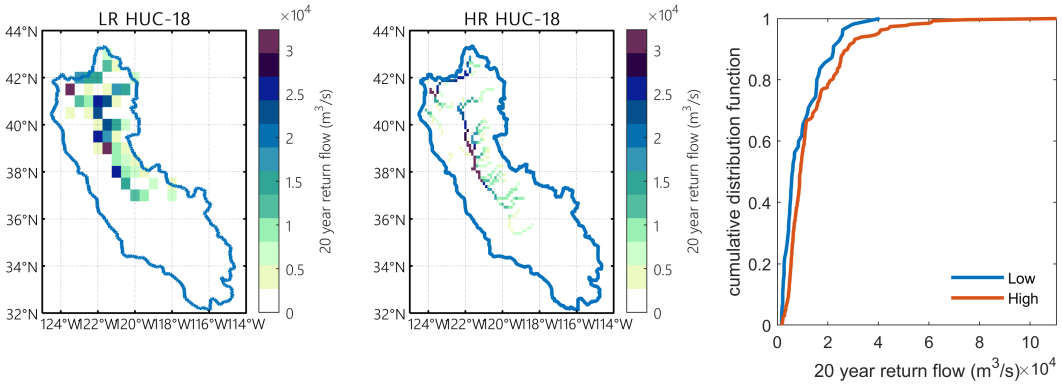

Figure S29. Same as Figure S12, only for the California (18) region.

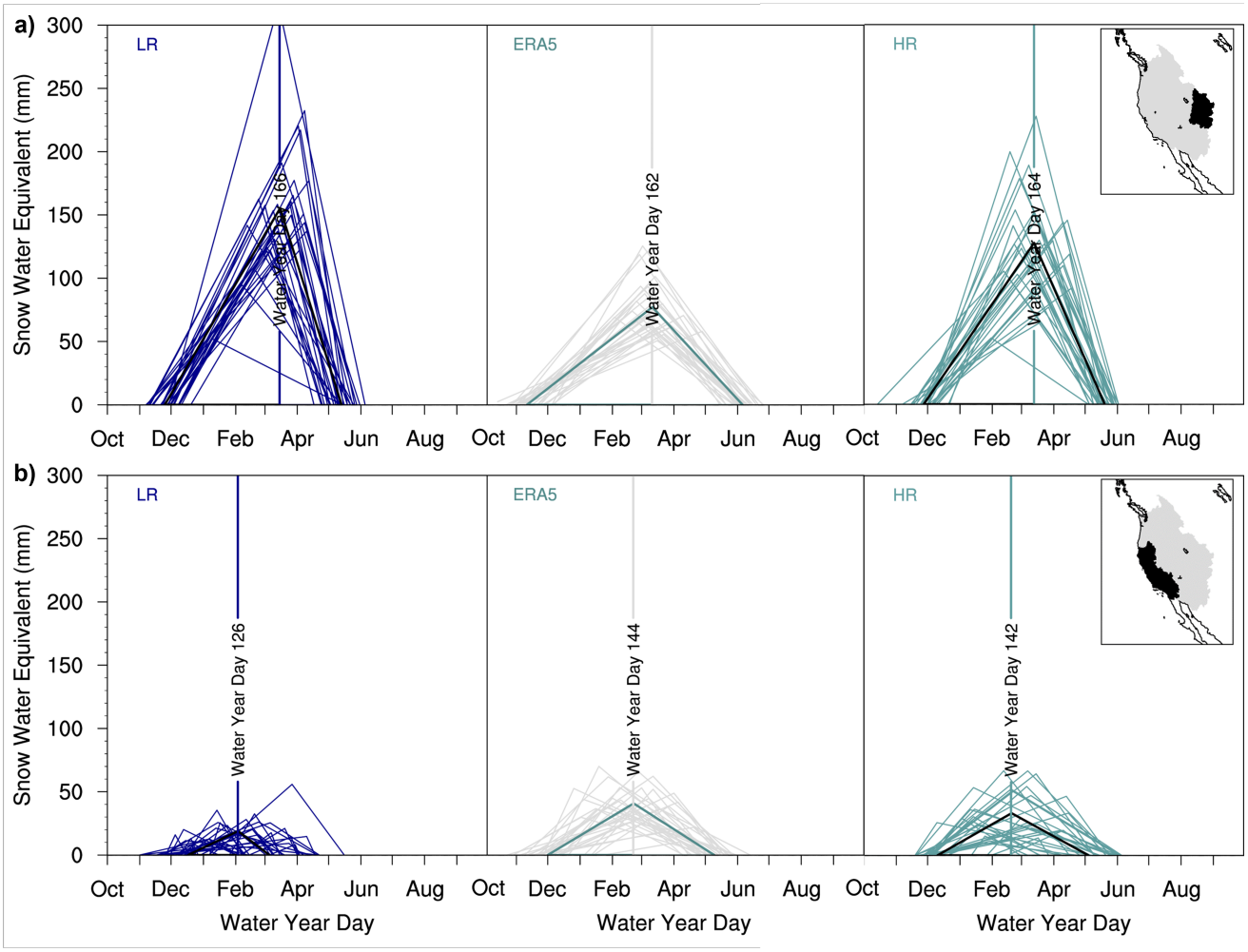

Figure S30. The seasonal snow cycle is characterized by its daily snow water equivalent (SWE) and linearly decomposed using the SWE triangle methodology to assess two western United States mountainous hydrologic units, a) California and b) Upper Colorado, for the E3SM low-resolution (LR, 1.00°, blue) and high-resolution (HR, 0.25°, aquamarine) simulations spanning 1985-2014 with the climatological average SWE triangle represented in black. ERA5 is shown in gray.

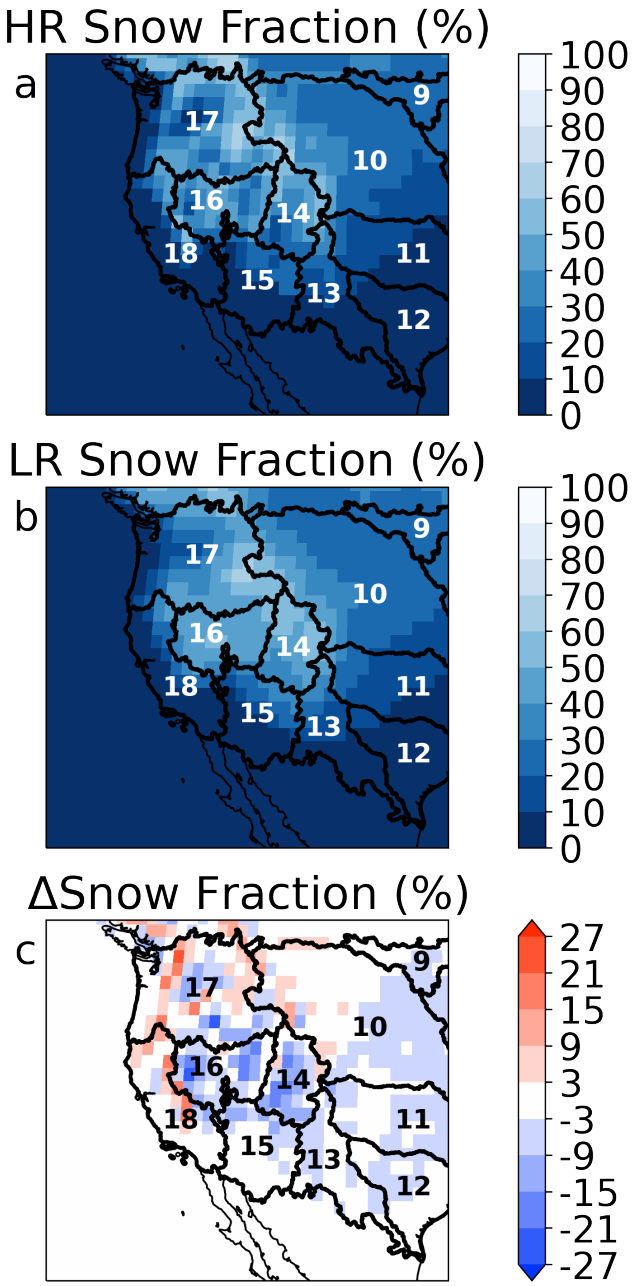

Figure S31. Fraction of total annual mean precipitation falling as snow for HR (a), LR (b), and their difference (c). All panels have units of percent.